Journal of Power Sources 215 (2012) 69–76

Contents lists available at SciVerse ScienceDirect

Journal of Power Sources

journal homepage: www.elsevier.com/locate/jpowsour

Experimental study on performance of a planar membrane humidifier for a proton exchange membrane fuel cell stack

Jenn Jiang Hwang [a,*], Wei Ru Chang [b], Jenn Kun Kao [a], Wei Wu [c]

[a] Department of Greenergy, National University of Tainan, Tainan 700, Taiwan
[b] Department of Landscape Architecture, Fu Jen Catholic University, Taipei, Taiwan
[c] Department of Chemical Engineering, National Cheng Kung University, Tainan, Taiwan

HIGHLIGHTS

- The water recovery ratio represents well the humidification performance of a membrane humidifier.
- The DPAT of the membrane humidifier decreases with increasing the wet inlet dew point.
- The stack–humidifier assembly is 10% less than the stack in the electrochemical performance.
- The stability and reliability of the membrane humidifier are acceptable.

ARTICLE INFO

Article history:
Received 23 March 2012
Received in revised form
20 April 2012
Accepted 21 April 2012
Available online 8 May 2012

Keywords:
Fuel cell
Membrane humidifier
Dew point approach temperature
Water recovery ratio

ABSTRACT

Experiments are conducted to evaluate the performance of a planar membrane humidifier for a PEM fuel cell stack. The humidification performance of the humidifier adopted here includes the dew point approach temperature (DPAT), water recovery ratio (WRR), and water vapor transfer rate (WVTR). Parametric studies involve the dry inlet temperature, the wet inlet dew point, and the flow rate across the humidifier. Results show that increasing the flow rate across the humidifier linearly increases its pressure drop. However, the DPAT increases sharply at high flow rates (>350 SLPM) due to the inadequate WVTR limited by the humidifier size. In addition, increasing the wet inlet dew point reduces the humidification performance by increasing the DPAT and reducing in the WRR. Moreover, an increase in the dry inlet temperature could reduce the DPAT at the low flow rate of 100 SLPM, but does not affect the DPAT at the high flow rate of 450 SLPM. Furthermore, the electrochemical performance of the stack–humidifier assembly is only 10% less than that of the stack tested on a commercial test station. Stability test reveals a satisfactory reliability of the present membrane humidifier as well.

1. Introduction

Fuel cell systems are being used as power sources in a wide variety of applications. They have been used as vehicular propulsion, stationary power plants in buildings and residences, and portable power in video cameras, computers, smart phones and the like.

Among various types of fuel cells, proton exchange membrane (PEM) fuel cells show most promise to replace the internal combustion engines for vehicular application since they could deliver high power density and operate at a low temperature, allowing for immediate startups and fast responses to changes in the power demand. However, a critical requirement of PEM fuel cells is to maintain high water content in the membrane electrolyte to ensure high proton conductivity. Lower water content in the membrane electrolyte would lead to a higher resistance of proton conduction, thus resulting in a higher ohmic loss. This not only reduces the system efficiency but also damages and thus shortens lifetime of the membranes. Therefore, it should provide a means for maintaining the fuel cell membranes in the moist condition [1].

The humidification technology of a PEM fuel cell has been developed for decades. The state-of-the-art technologies for humidification of a PEM fuel cell include passing feeding gas through hot water as a wet stream of fine bubbles, injecting water directly into the feeding gas stream, or recycling the moisture from the cathode exhaust to the cathode inlet stream. In the first scheme, water transfer is achieved by heating the water bath to a set temperature while bubbling the reactant gases through the hot water [2–4]. As the gases rise through the water, they take up water vapor and thus are humidified. The amount of water transferred to the gas stream depends on the water temperature, the contact area

* Corresponding author. Tel.: +886 62600321; fax: +886 62602596.
E-mail address: azaijj@mail.nutn.edu.tw (J.J. Hwang).

0378-7753/$ – see front matter © 2012 Elsevier B.V. All rights reserved.
doi:10.1016/j.jpowsour.2012.04.051

of the water–air interface, and the contact time of the air bubbles with the water [5]. The bubbler humidifier is quite simple in technique, but several drawbacks limit its commercial application including unknown humidification, and inability to provide real time change in humidity. In general, it is impractical beyond the laboratory scale. The second method is to inject water directly into the fuel cell, or the feeding line leading into the manifold [6]. In this design, liquid water is preheated to fuel cell operational temperature and then pumped directly into the fuel cell reactant streams. It is suitable for a fuel cell stack of large power [7], but is not efficient for a smaller power system. Similar systems would be available by using a steam generator to provide hot saturated air for the fuel cell, however without an abundant heat source significant power losses would be expected in the production of steam.

The humidification devices for recycling the humidity in the fuel cell system include the enthalpy wheel and the membrane humidifier. The former is an active method originated from desiccant wheel dehumidification [8–10]. By passing two counter-flow streams through a rotating honeycomb ceramic, the damp exhaust from the fuel cell cathode passes through one side putting down moisture while the dry inlet stream passes through another side picking up moisture. This technology needs power to drive the rotating drum together with control, which yields a parasitic loss and adds to system complexity under transient operation. In addition, the leakages as well as the cross-flow are likely to occur. In contrast, the membrane humidifier does not require an extra parasitic power to drive such as a rotating motor, a water pump or a controller. In addition, it is light in weight, simple in design, and has no moving parts that frequently lead to sealing problems. This is the reason why the membrane humidifier has received a lot of attention in application of PEM fuel cell systems [11–20]. In general, the membrane humidifiers could fall into two categories, i.e., planar and tubular. In the tubular design, dry gas flows through the hollow fiber bundles and gets humidified by adsorbing the water of the moisture interface of the hollow fiber membrane [21]. As for the planar membrane humidifier, flat membrane sheets separate the cathode wet exhaust stream incoming from the fuel cell from the dry inlet stream, which works similarly to a plate and frame heat exchanger. Note that the membranes could be made from fluorinated materials (such as perfluorosulfonic acid, PFSA) or other non-fluorinated materials (such as hydrocarbon polymers).

This paper deals with a planar membrane humidifier, which recycles heat and humidity from the cathode exhaust of the fuel cell system. In this work, a prototype of membrane humidifier is designed, fabricated, and tested thereafter. The humidification performance of the membrane humidifier such as the dew point approach temperature (DPAT), water recovery ratio (WRR), and water vapor transfer rate (WVTR) is evaluated under various flow and humidity conditions. Basically, these performance parameters are dependent on but complementary to each other. They provide the information of humidifier efficiencies from different aspects as well as illustrate the transport phenomena of water vapor in the humidifier quantitatively and qualitatively. Then, the membrane humidifier and the PEM fuel cell stack are integrated into a compact unit in order to reduce the redundant pipes and fitting and save space [22–25]. In addition, the electrochemical performance of a stack–humidifier assembly is examined under real operational conditions, which compares to the polarization curve of the fuel cell stack that is obtained from the commercial test station. Finally, the durability test is carried out to assess the reliability and stability of the planar membrane humidifier integrated into a PEM fuel cell stack.

2. The experiment

2.1. Experimental setup

The experimental setup is shown in Fig. 1. Air from the laboratory is compressed into the test section, which is divided into a dry stream and a wet stream by using a tee adaptor. For the dry stream, the compressed air passes through a mass flow controller (MFC) to regulate the flow rate. It is then heated in a gas-heating chamber to the desired temperature before entering the dry inlet port of the membrane humidifier. For the wet stream, the compressed air passes through another MFC, another gas heater, and then enters an evaporator. In the evaporator, the injecting water is flash evaporated on a dry surface and the resulting steam engaged with the heated air stream. The temperature of the air–vapor mixture is raised to entrain all of the steam being generated, which results in a saturated gas stream exiting the evaporator at its dew point. In addition, a heated flexible tube for the output gas stream avoids condensation of the humid gas. The heated flexible tube has an interior of Teflon, which is then wrapped with a heater, followed by insulation and a sheath. It has an internal thermocouple for monitoring the humidifier and a high temperature cutout switch for protection. Closed loop control of humidity based on a signal from a humidity sensor ensures accurate control of humidity before entering the humidifier. As compared with the conventional bubbler humidifier, the present technology provides the ability to directly control the dew point of the gas stream on a real time basis

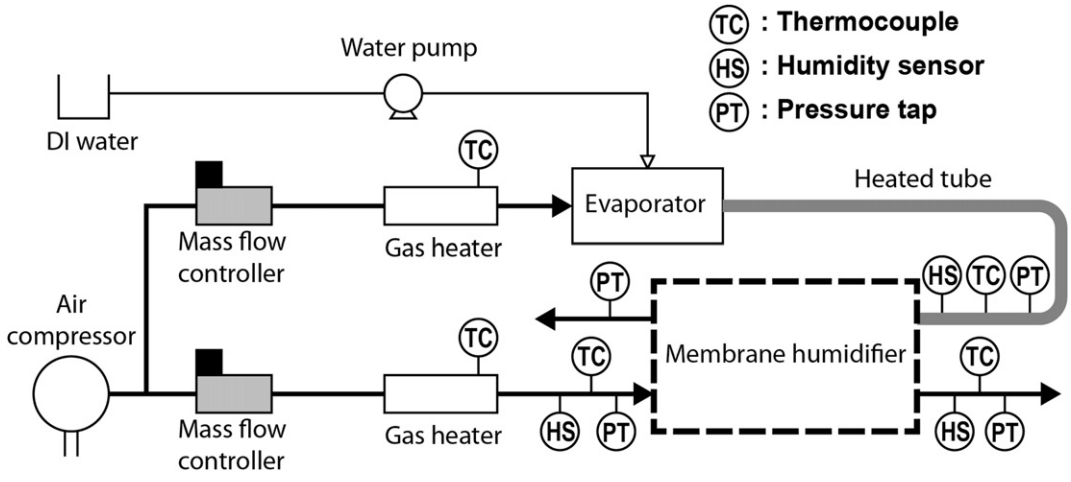

Fig. 1. Experimental setup.

Table 1
Instruments for experimental measurements.

Data	Model	Manufacturer
Pressure	SENSOTEC FPA1000	Honeywell
Temperature	Thermocouple (T type)	Omega
Mass flow rate	Models 5853E	Brooks
Relative humidity	HumiTrac	General eastern
Data logger	DA100/DS600	Yokogawa

in addition to entrain significantly more water into the gas stream, which enables a high flow of humid gas with quick response.

Table 1 shows the instruments for the measurement of the performance of the humidifier. The temperature of the gas stream is measured by using the copper–constantan thermocouples (T type) [26]. The humidity sensor used is the General Eastern HumiTrac™ series relative humidity/temperature transmitter. They are placed through a hole drilled in a pipefitting plug. For the pressure-drop measurements across the membrane humidifier, four pressure taps located at inlets and outlets of two streams are connected to a signal-receiving micro-differential pressure transducer, which are subsequently amplified by a conditioner and then recorded in a digital readout (Yokogawa) [27–30].

2.2. Membrane humidifier

Fig. 2(a) and (b) gives the photos of the membrane humidifier and the assembly of the fuel cell stack and the membrane humidifier, respectively. The fuel cell stack used herein is a customized

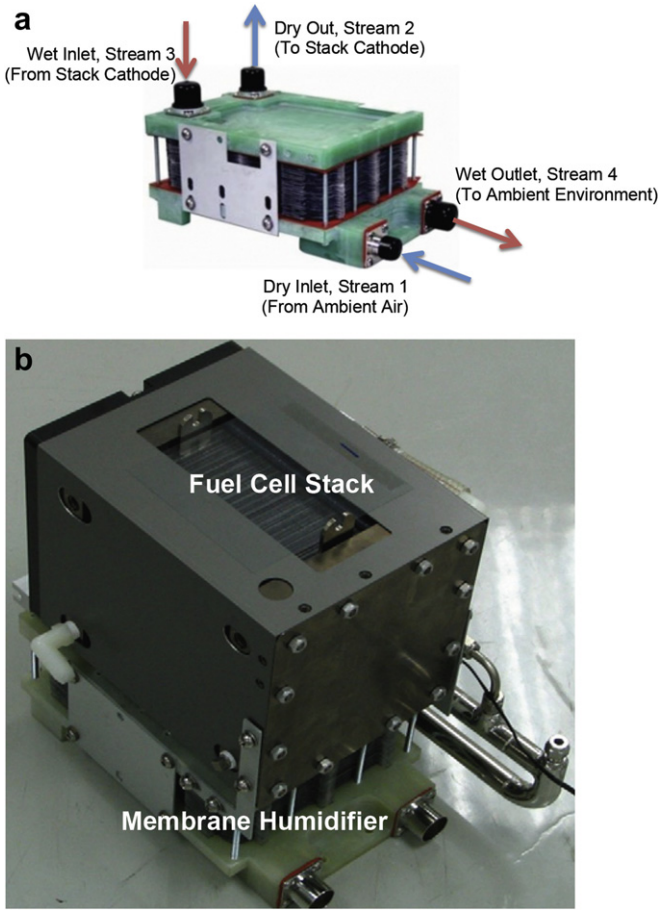

Fig. 2. (a) Membrane humidifier, (b) assembly of a PEM fuel cell stack and a membrane humidifier.

product [31,32]. It has an active area of 150 cm^2 and connects 74 cells in series. The membrane humidifier consists of a number of humidifier modules connected in series like the assembly of a fuel cell stack. The structure of the humidifier module (i.e. bi-flow plates) is made of an engineering thermoplastic material of polyurethane, which will not release compounds that adversely affect the fuel cell. All humidifier modules are screwed tightly between two end plates that are made of glass-fiber reinforced plastic (GFRP).

The working principle of the membrane humidifier is further depicted schematically in Fig. 3. Dry gas entering the humidifier (stream 1) gains heat and humidity through the fuel cell system before entering the fuel cell (stream 2). In the fuel cell environment, the gas stream has decrease in oxygen content as the fuel cell reaction occurs; as well the stream is likely to increase in water and heat content before exiting the fuel cell as exhaust (stream 3). This hot and wet exhaust stream enters the humidifier where the heat and humidity in the stream will be transported back to the inlet stream, before exiting the system at stream 4. As further seen from Fig. 3, the repeated humidifier module consists of a bi-flow plate, two diffusion layers and a membrane. The bi-flow plate made of polyurethane is 2.5 mm in thickness. Parallel channels are machined on both sides of the bi-flow plate, which convey the wet stream from the cathode of the fuel cell to an exhaust and the dry stream from ambient gas to the cathode inlet of the fuel cell, respectively. These two streams are in cross-flow direction. The channels are 1 mm in depth, 2 mm in width, and separated by 1.5 mm lands. The flow enters and exits each side through adaptors and then spreads out to the parallel channels. Note that a counter-flow of the gas streams can also be used to facilitate a transport of water vapor from wet gas stream to the dry gas stream. For a fuel cell humidification application, the water transfer effectiveness requirement is typically low. As a result, there is little expected performance difference between counter-flow and cross-flow design [33].

The membrane used herein is a conventional extruded PFSA film, Nafion® 115, which is 127 μm in thickness and 1100 in equivalent weight. When water strikes an exposed sulfonic acid group on the surface of the membrane, the surface sulfonic acid group binds the water initially. Additional groups deeper in the wall have less water attached to them, and consequently a higher affinity for water. Water molecules absorbed onto the surface of the

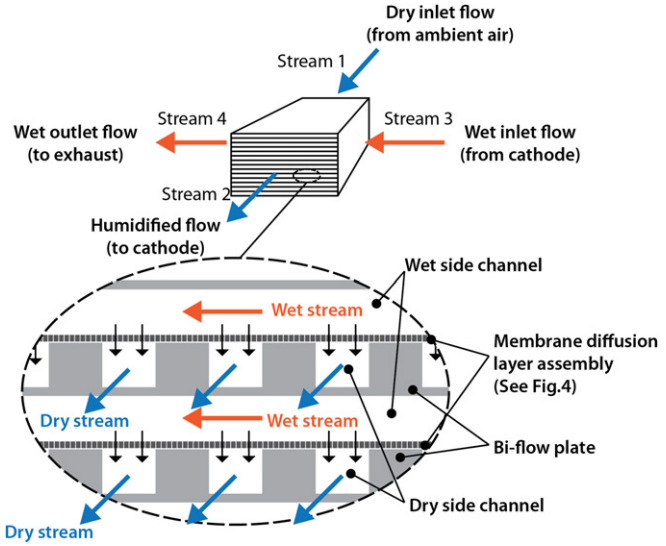

Fig. 3. Schematic drawing of the membrane humidifier.

membrane are therefore quickly passed on to underlying sulfonic acid groups, until the water reaches the opposite side. The water molecule then pervaporates into the surrounding medium. This process continues until the water vapor pressure gradient across the membrane is eliminated. If a very low water vapor pressure is maintained one side of the membrane surface, water will stream across the membrane very quickly.

As shown in Fig. 4, a membrane sheet of 150 cm^2 in the active surface area is sandwiched between two diffusion layers, which forms a membrane–diffusion layer assembly. The entrance and exit areas of the membrane are covered with a thin sheet of water and air-impermeable polyimide film so that only the channel areas are exposed to the flow, eliminating any entrance and exit effects on water transfer and allowing the flow to become fully developed. The diffusion layers are made from non-woven fabrics, which are resilient and gas permeable. It has a thickness of 0.1 mm, and a porosity of 85%. The pore size in the diffusion layers is in the range of 1–50 μm. In the present design, the channel area ratios of the bi-flow plate are in the range of 75–85%, which are chosen to maximize membrane area utilization under the lands and minimize the intrusion of the membrane or other structures into the flow channels. Additional favorable conditions have been controlled wherein a flow of gas through the channels is laminar, which might minimize a pressure drop through the channels and maximize the water vapor transport through the diffusion layers and the membrane.

3. Data reduction of performance matric

Fig. 4 represents a general behavior of water partial pressure (P_w) across a humidifier module. The wet gas stream is fed to one side of the membrane whereas the dry gas stream is fed to another side of the membrane. A molecular transport of water from the wet-side channel to the dry-side channel includes several transport modes. A convection mass transport of water vapor occurs in the channels. A diffusion transport occurs through the diffusion layers. Water vapor is also transported by diffusion through the membrane. In addition, water is transferred through the membrane by hydraulic forces due to the pressure difference existing between the wet-side channels and the dry-side channels. Moreover, temperature difference between the wet-side channels and the dry-side channels may also affect the transport of water there between. That is an enthalpy exchange between two streams would be associated with water flux. It is interesting to note that the membrane humidifier is lack of water drag of proton from the anode to the cathode as compared to the water transports in an active PEM fuel cell.

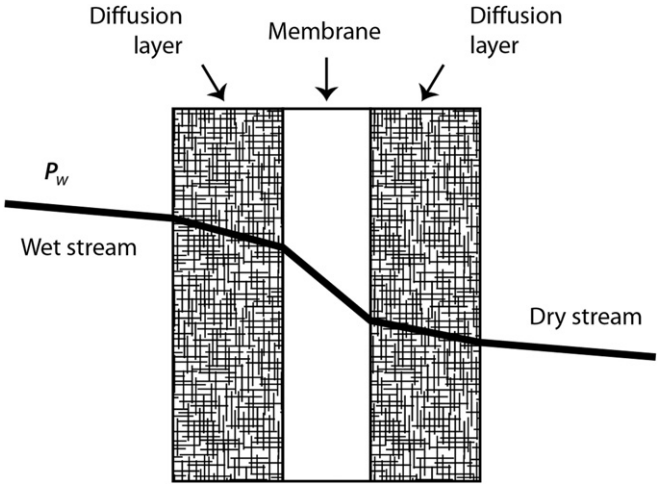

Fig. 4. Conception of pressure distribution across the membrane–diffusion layer assembly.

3.1. Water vapor transfer rates

The performance of a humidifier is usually gauged by the amount of water it transfers. The water vapor transfer rate is an absolute measure that is simply the rate of water mass transferred across the membrane. It can be determined by subtracting the water mass flow rate in the dry inlet flow (stream 1) from that in the dry outlet flow (stream 2).

$$\mathrm{WVTR} = \dot{m}_{\mathrm{H_2O,s2}} - \dot{m}_{\mathrm{H_2O,s1}} = (a_{s2} - a_{s1}) \times \dot{v} \quad (1)$$

where a is absolute humidity (g m^{-3}) measured at the inlet and outlet ports of the dry gas stream, and $\dot{v}$ is the volume flow rate (m^3 s^{-1}) across the membrane humidifier. It is a proper index for comparing identical humidifiers over a range of flow and/or humidity conditions. To compare different humidifiers over different flow and/or humidity conditions, however, the water flux J would be a better quantity, which takes into account the humidifier size (and hence module number n and membrane area A) that the water is transferring through:

$$J = \frac{\dot{m}_{\mathrm{H_2O,s2}} - \dot{m}_{\mathrm{H_2O,s1}}}{n \times A} \quad (2)$$

3.2. Dew point approach temperature

The cathode inlet dew point (dry outlet dew point) is usually used as a specification for system humidification. However, it provides little information regarding humidification performance. Basically, a measure to quantify the performance of a humidifier should address how well a humidifier performs compared to how well the device could potentially perform. Therefore, desirable performance of a humidifier occurs when the water vapor transport rate is maximized or, conversely, when the dew point of the dry outlet stream approaches that of the incoming wet stream. The dew point approach temperature is therefore defined as the dew point difference between the cathode exhaust stream entering the humidifier and the humidified stream going to the stack. In another word, DPAT is a gauge of how close the dry outlet dew point comes to the wet inlet dew point of a humidifier, i.e.,

$$\mathrm{DPAT} = T_{\mathrm{wet-in\ dew\ point}} - T_{\mathrm{dry-out\ dew\ point}} \quad (3)$$

For example, if the cathode exhaust entering the humidifier has a dew point of 65 °C, and it generates a cathode inlet dew point of 58 °C, the humidifier would have a 7 °C in the dew point approach temperature. In an ideal humidifier, the DPAT should be zero.

3.3. Water recovery ratio

The water recovery ratio is an important humidification performance based on the moisture transfer rate. It is a latent effectiveness similar to the sensible (temperature) effectiveness in a heat exchanger. The non-dimensional parameter WRR describes how much water is transferred to the dry outlet compared to the maximum amount of water that could be transferred, which would be the water content in the wet stream. It can be demonstrated as the following equation:

$$\mathrm{WRR} = \frac{\dot{m}_{\mathrm{w2}} - \dot{m}_{\mathrm{w1}}}{\dot{m}_{\mathrm{w3}}} = \frac{\dot{m}_{\mathrm{a2}} \times (\omega_2 - \omega_1)}{\dot{m}_{\mathrm{a2}} \cdot \omega_{\mathrm{w2}}} \quad (4)$$

where ω is the humidity ratio (g g^{-1})of the air–vapor mixture,

$$\omega = \frac{P_w}{P - P_w} \cdot \frac{M_w}{M_a} \quad (5)$$

Since the wet stream and the dry stream across the humidifier have the same flow rates, i.e., $\dot{m}_{a1} = \dot{m}_{a2}$, the water recovery ratio can be reduced to:

$$\mathrm{WRR} = \frac{\omega_2 - \omega_1}{\omega_3} \times 100\% \quad (6)$$

The stream 1 is generally ambient and has little water content. In this work, the air supply is pre-dried, so ω_1 is zero. In a fuel cell system, the stream 3 will be exiting the fuel cell as exhaust. It will likely be saturated with water at the fuel cell operating temperature and would be a donator of water vapor in the operation of the humidifier. In this work, the dew point of the stream 3 varies from 50 °C to 80 °C. The stream 2 will gain moisture content and heat and its humidity ratio ω_2 indicates how much moisture the humidifier has received.

4. Results and discussion

4.1. Pressure drop

Fig. 5 shows the pressure drops as a function the flow rates across the membrane humidifier. In this figure, the open squares represent the pressure drop across the wet-side channels while the open triangles are the pressure drops across the dry-side channels. The pressure drops for these two streams are largely identical. The solid circles are the sum of pressure drops across the wet-side channels and the dry-side channels, which represent the total pressure loss due to the membrane humidifier in an operating fuel cell system. It is clearly seen from this figure that the total pressure drop across the membrane humidifier is increased with increasing the airflow rate, meaning that higher drags in the membrane humidifier require more pumping power driving the cathode stream under higher power conditions.

4.2. Water transport performance

Figs. 6–11 show the water transport performance of the planar membrane humidifier. All of the results are discussed in terms of the performance parameters of DPAT, WVTR, and WRR under various flow and humidity conditions.

The effect of flow rate across the humidifier on the humidification performance of the humidifier is given in Figs. 6–8. In this experiment, the dew point of the wet inlet stream simulating the cathode outlet stream is controlled at 60 °C, while the dry inlet

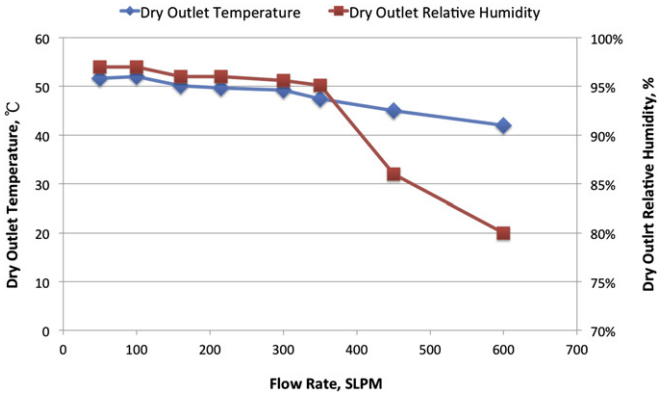

Fig. 6. Effect of flow rate on the dry outlet temperature and relative humidity, wet inlet dew point: 60 °C.

stream entering the membrane humidifier has a temperature of 25 °C. Fig. 6 shows the variation of temperature (solid diamonds) and relative humidity (solid squares) of the dry outlet flow (stream 2) at different flow rates across the humidifier. It is seen from this figure that the dry outlet temperature decreases linearly with the flow rates. As for the relative humidity, the dry outlet flow keeps a high level of the relative humidity (>95%) as the flow rate is less than 350 SLPM. This is because the water transferred from the wet stream is enough to humidify the dry stream. However, there is a sharp drop in the relative humidity as the flow rate increases from 350 to 600 SLPM. The reason may be illustrated by the results in Fig. 7, which shows the effect of flow rate on the WVTR as well as the WRR under the operational conditions. It is clearly seen from in this figure, as the flow rates are less than 350 SLPM, the WVTR increases with increasing the flow rate. When the flow rate increases from 350 to 600 SLPM, the WVTR keeps constantly almost, i.e. 4.1 ± 0.1 g s^{-1}. Although, a high flow rate enhances the convection mass transfer from the channels to the membrane surface, there is still a bottleneck for water vapor diffusion along the membrane thickness, which is related to the membrane employed. In general, the capacity of water vapor transmission across the membrane depends on the permeation of the membrane as well as the diffusion area of the membrane. The above results has explicitly indicated that the present prototype of membrane humidifier is capable of humidifying the dry flow up to 350 SLPM, which can support a PEM fuel cell stack of a nominal power about 6.5 kW with a cathode stoichiometry of 2.5. Basically, increasing the humidifier size (membrane area, and module number) as well as improving the water vapor permeation of the membrane could

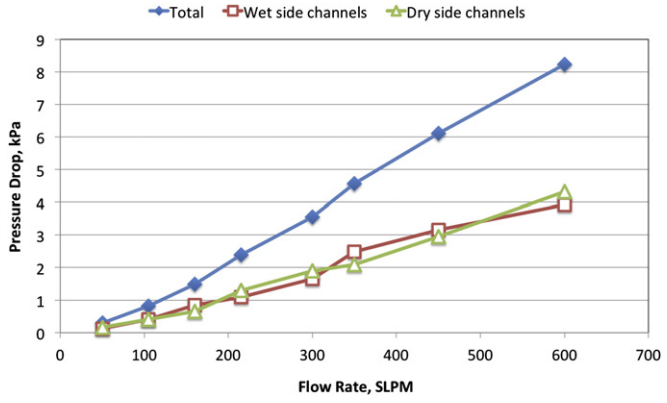

Fig. 5. Effect of flow rate on the pressure drop across the membrane humidifier.

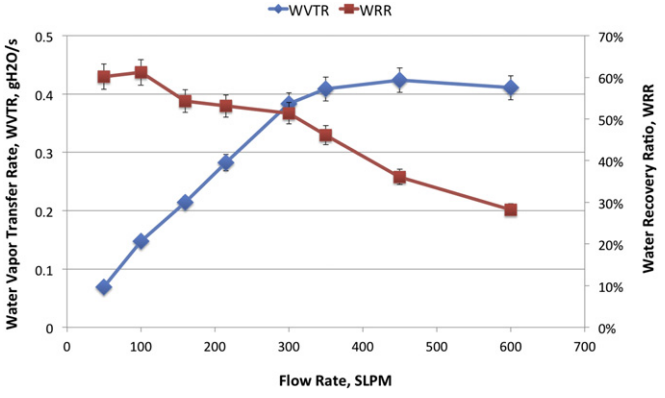

Fig. 7. Effect of flow rate on the water vapor transfer rate and the water recovery ratio of the dry outlet stream, wet inlet dew point: 60 °C.

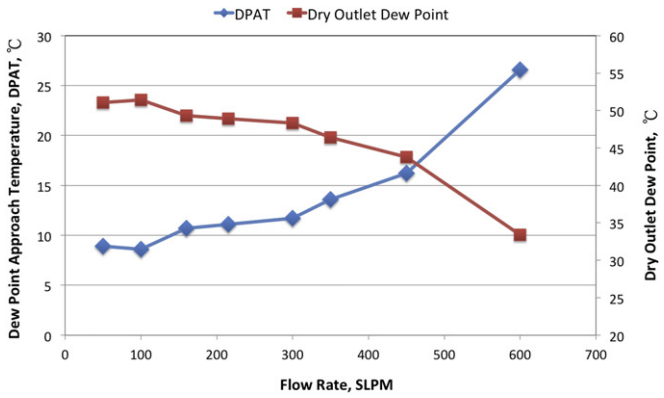

Fig. 8. Effect of flow rate on the dew point and the dew point approach temperature of the dry outlet stream, wet inlet dew point: 60 °C.

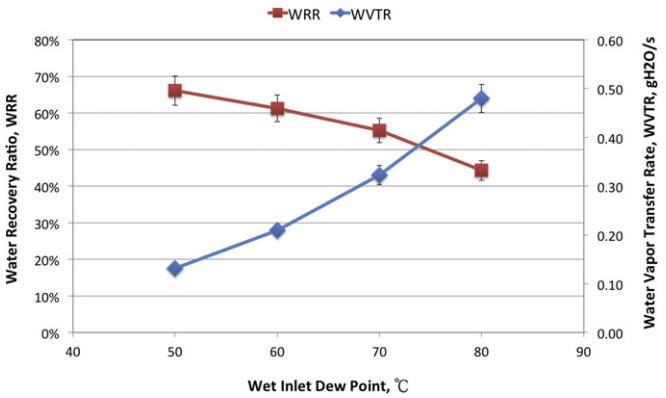

Fig. 10. Effect of wet inlet dew point on the WTR and WRR, dry inlet temperature 25 °C; relative humidity: 0; flow rate: 100 SLPM.

improve the dry outlet relative humidity at high flow rates. As for the WRR, it is increased with increasing the flow rate across the membrane humidifier. Fig. 8 gives another important parameter to evaluate the humidification performance of the humidifier, i.e. the DPAT (solid diamonds). It is seen from this figure that the DPAT slightly increases with increasing the flow rates for the flow rate lower than 350 SLPM. As for the flow rate is greater the 450 SLPM, similarly, the DPAT increases abruptly. The DPAT is as high as 27 °C at the flow rate of 600 SLPM, which reflects its poor water recovery ratio about 30% (Fig. 7).

Figs. 9and 10 show the effect of wet inlet dew point on the humidification performance of the membrane humidifier. In this experiment, the dry inlet temperature is controlled at 25 °C and the flow rate across the membrane humidifier is fixed at 100 SLPM. It is seen from Fig. 9 that the dry outlet dew point is increased with increasing the wet inlet dew point. Note that a higher wet inlet dew point (cathode exhaust) means a higher fuel cell operation temperature that requires a higher dry outlet dew point. In addition, a higher wet inlet dew point always comes with a higher dry outlet inlet dew point. Therefore, the humidifier with a higher dry outlet dew point does not mean a superior humidification performance here. Actually, the DPAT presented in Fig. 9 could compensate for using the dry outlet dew point alone, in which the humidification performance decreases in terms of DPAT as the wet inlet dew point increases, yet the actual dry outlet dew point increases. Fig. 10 gives another parameter of the WRR to explain the above phenomena. As shown in Fig. 10, the WRR is decreased with increasing the wet inlet dew point although a high wet inlet dew point enhances the WVTR from the wet side channels to the dry side channels. That is there is more room for water vapor to be transferred from the wet side channels to the dry side channels for a higher wet inlet dew point.

Fig. 11 shows the effect of the dry inlet temperature on the performance of the humidifier. In this figure, the wet stream has a dew point of 60 °C at the inlet, and the results of two flow rates, i.e., 100 SLPM and 450 SLPM, are compared. At the low flow rate of 100 SLPM, the DPAT increases with increasing the dry inlet temperature. That is a hot stream at the dry inlet is accompanied with a low DPAT, which can be explained by the fact that there is more water vapor in the wet stream transferred to the dry stream (solid diamonds). In contrast, at a high flow rate of 450 SLPM, the dry inlet temperature does not affect the DPAT essentially. Even with a significant latent potential between the wet stream and the dry stream, the abovementioned water vapor capacity of the membrane limits the water vapor transfer rate for higher volume flow rate across the humidifier.

4.3. Electrochemical performance of a stack–humidifier assembly

The last task of this work is to evaluate the electrochemical performance of the membrane humidifier when it integrates with a fuel cell stack. As shown in Fig. 2, the stack–humidifier assembly has a PEM fuel cell stack of 4.0 kW in nominal power.

Before assessing the electrochemical performance of the stack–humidifier assembly, it is important to know the polarization curve of the fuel cell stack, which serves as a benchmark to

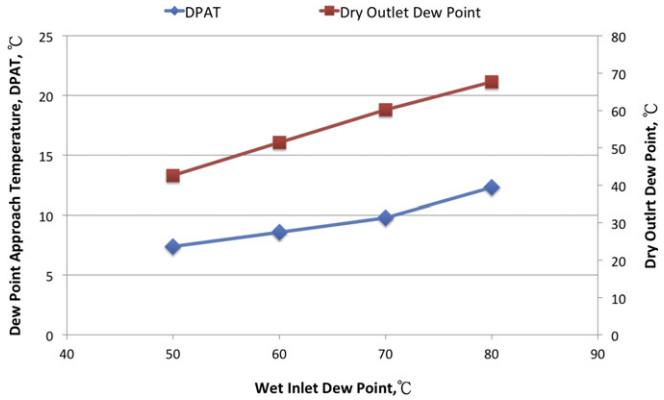

Fig. 9. Effect of wet inlet dew point on the dry outlet DP and DPAT, dry inlet temperature: 25 °C; relative humidity: 0; flow rate: 100 SLPM.

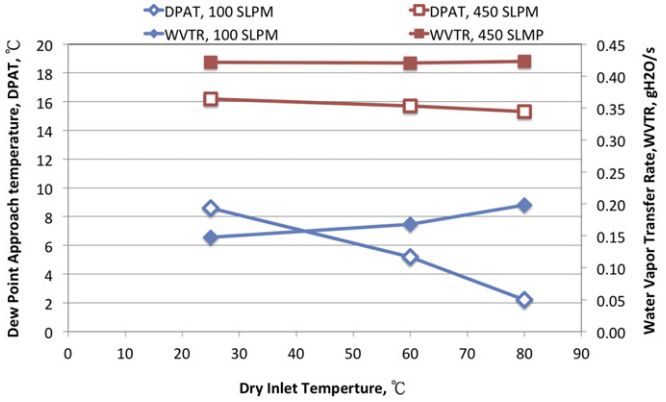

Fig. 11. Effect of dry inlet temperature on the dew point approach temperature and water vapor transfer rate under various flow rates, wet inlet dew point: 60 °C.

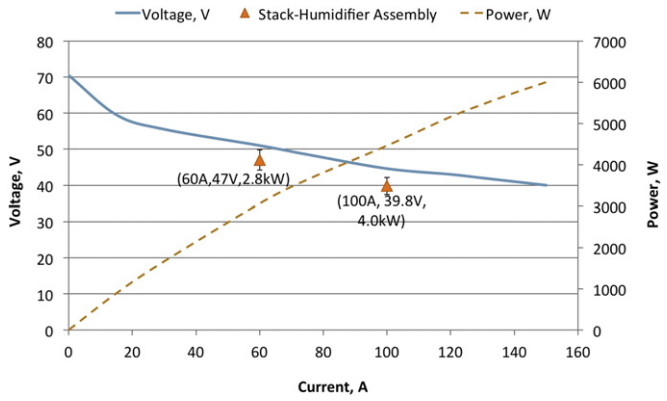

Fig. 12. Departure of the performance between the fuel cell stack test on the test station and the result obtained with the stack–membrane assembly.

compare with. The characteristic curves in Fig. 12 are the results obtained from the PEM fuel stack alone on a commercial test station (Greenlight), in which the flow and humidity conditions are well controlled. That is both the anode stream and the cathode stream are fully humidified (with relative humidity of 100%), the operational temperature of the fuel cell stack is controlled at 60 °C, and the cathode stoichiometric ratio is fixed at 2.5.

Two data points on Fig. 12 are the measurements of the stack–humidifier assembly under the extracted currents of 60 A and 100 A, respectively. In this circumstance, the saturated cathode exhaust humidifies the cathode inlet air, while the anode inlet stream is the dry hydrogen from the hydrogen tank. It is clearly observed from this figure that the power delivered by the stack–membrane assembly is slightly lower than the characteristic curves of the fuel cell stack. At the extracted current of 60 A, the stack–humidifier assembly delivers about 2.8 kW power. While the fuel cell stack has the potential to deliver 3.0 kW power at the same current. Similarly, at the current of 100 A, the power extracted from the stack–humidifier assembly is about 10% less than that of the fuel cell stack. Actually, the electrochemical performance of the membrane humidifier has been illustrated by the departure of power between the fuel cell stack and the stack–humidifier assembly at the same current. Additional stability test of the stack–humidifier assembly is conducted to ensure the reliability of the present membrane humidifier, which is shown in Fig. 13. The stack–humidifier assembly is operated under the constant power constraint of 4.0 kW, while the stack temperature and the cathode stoichiometric ratio are fixed at 60 °C and 2.5, respectively. Evidently, the test results have revealed that the stack–humidifier assembly displays reliable operation without any failure for over

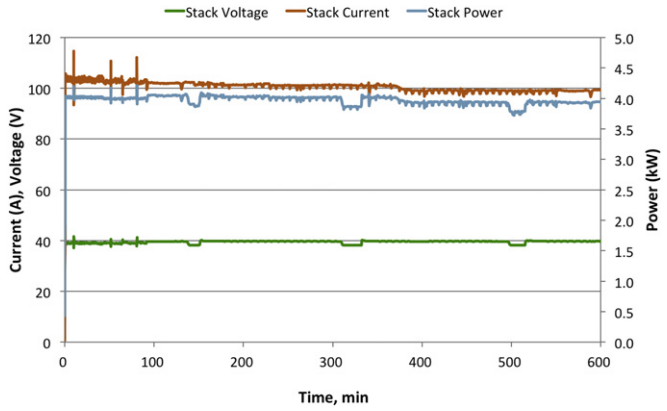

Fig. 13. Stability test of the fuel cell stack–membrane humidifier assembly at 4.0 kW.

10-h test. Generally speaking, the above results have signified the stability and reliability of the present membrane humidifier.

5. Conclusions

In this work, a prototype of planar membrane humidifier is fabricated and its performance is evaluated by varying the flow and humidity conditions. The humidification performance of a membrane humidifier is discussed in terms of the parameters of dew point approach temperature (DPAT), water recovery ratio (WRR) and water vapor transfer rate (WVTR). Based on the test results, major findings are concluded below:

1. The DPAT slightly increases with increasing the flow rates for the flow rate <350 SLPM. After the flow rate >350 SLPM, the DPAT increases sharply because of the limitation of the WVTR by the size of the membrane humidifier.
2. At the low flow rate of 100 SLPM, the humidifier performs better at a higher dry inlet temperature, which reflects on the lower DPAT and a higher WVTR. In contrast, the dry inlet temperature does not affect the DPAT at the high flow rate of 450 SLPM, in which the WVTR across the membrane does not alter as well.
3. At the constant current conditions of 60 A and 100 A, the electrochemical performance of the stack–humidifier is about 10% less than that of the fuel cell stack alone, in which the stack is tested on a commercial test station to well control the flow and humidity conditions.
4. The stack–humidifier assembly displays a proper operation without any failure for over 10-h electrochemical test, indicating that the stability and reliability of the present membrane humidifier might be satisfactory.

Acknowledgements

The authors would like to acknowledge the Natural Science Council (NSC) of Taiwan for financial support under contract number NSC-100-2212-E-013, as well as equipment support from APFCT Technologies (Taiwan).

References

[1] Fuel Cell Handbook, seventh ed. EG&G Technical Services, Inc., 2004.
[2] N. Rajalakshmi, P. Sridhar, K.S. Dhathathreyan, J. Power Sources 109 (2002) 452.
[3] R. Glises, D. Hissel, F. Harel, M.C. Pera, J. Power Sources 150 (2005) 78.
[4] G. Vasu, A.K. Tangirala, B. Viswanathan, K.S. Dhathathreyan, Int. J. Hydrogen Energy 33 (2008) 4640.
[5] B. Thorat, A. Shevade, K. Bhilegaonkar, R. Aglawe, U. Parasu Veera, S. Thakre, A. Pandit, S. Sawant, J. Joshi, Trans. IChemE 76 (1998) 823.
[6] D.L. Wood, J.S. Yi, T.V. Nguyen, Electrochim. Acta 43 (1998) 3795.
[7] H.J. Seung, L.K. Seok, S.K. Min, Y. Park, W.L. Tae, J. Power Sources 170 (2007) 324.
[8] Emprise Corporation, "Humidicore specifications", retrieved January 2007, from: http://www.humidicore.com/.
[9] X.S. Lao, H.S. Ma, J.T. Zhao, H. Zeng, W. Zhuge, Y. Zhang, J. Fuel Cell Sci. Technol. 6 (2008) 014501.
[10] A. Casalegno, S. De Antonellis, L. Colombo, F. Rinaldi, Int. J. Hydrogen Energy 36 (2011) 5000.
[11] D. Picot, R. Metkemeijer, J.J. Bezian, L. Rouveyre, J. Power Sources 75 (1998) 251.
[12] D. Chen, W. Li, H. Peng, J. Power Sources 180 (2008) 461.
[13] S. Takahiro, Gas humidifier and method for the same, Japan patent #JP2004028490. 2004-01-29.
[14] S. Hiroshi, K. Yoshio, S. Mikihiro, K. Toshikatsu, Humidifier, Japan patent #JP2005098695. 2005-04-14.
[15] S. Masaharu, I. Tamio, H. Takahiro, Hollow fiber membrane module and humidifier of fuel cell, Japan patent #JP2005034715. 2005-02-10.
[16] S. Tanaka, Hollow fiber membrane humidifier, Japan patent #JP2005158517. 2005-06-16.
[17] R.H. Barton, B. Wells, J.A. Ronne, Plate and frame fluid exchanging assembly with unitary plates and seals, US patent #6171374. 2001-01-09.
[18] A. Mossman, Membrane exchange humidifier, US patent application #2005191530. 2005-09-01.
[19] P. Cave, W. Merida, J. Power Sources 175 (2008) 408.

[20] R. Huizing, M. Fowler, W. Mérida, J. Dean, J. Power Sources 180 (2008) 265.
[21] Permapure Inc. “Perma pure fuel cell website.” retrieved January 2012, from: http://www.permapure.com/FC/.
[22] C.Y. Chow, B.M. Wozniczka, Electrochemical fuel cell stack with humidification section located upstream from the electrochemically active section, US patent 5382478, 1995.
[23] M.C. Tonkin, M.E. Schuchardt, M.A Young, A humidifying gas induction or supply system, WIPO patent WO/2001/011216.
[24] H. Chizawa, Y. Ogami, K. Saito, M. Ueno, Solid polymer type fuel cell system, European patent application EP1030396 A1, 2000.
[25] H.H. Voss, R.H. Barton, B.W. Wells, J.A. Ronne, H.A. Nigsch, Solid polymer fuel cell system and method for humidifying and adjusting the temperature of a reactant stream, US patent 6106964, 2000.
[26] J.J. Hwang, G.J. Hwang, R.H. Yeh, C.H. Chao, J. Heat Transfer 124 (2002) 120.
[27] J.J. Hwang, T.M. Liou, Int. J. Heat Mass Transfer 38 (1995) 3197.
[28] J.J. Hwang, D.Y. Lai, Int. J. Heat Mass Transfer 41 (1998) 979.
[29] J.J. Hwang, T.M. Liou, J. Heat Transfer 116 (1994) 912.
[30] J.J. Hwang, C.S. Cheng, J. Heat Transfer 121 (1999) 683.
[31] J.J. Hwang, D.Y. Wang, N.C. Shih, J. Power Sources 141 (2005) 108.
[32] J.J. Hwang, W.R. Chang, J. Power Sources 207 (2012) 111.
[33] J.J. Hwang, S.D. Wu, L.K. Lai, J. Power Sources 161 (2006) 240.